PAPER

Deep double descent: where bigger models and more data hurt*

Journal of Statistical Mechanics: Theory and Experiment
An IOP and SISSA journal

PAPER: ML 2021

Deep double descent: where bigger models and more data hurt*

Preetum Nakkiran[1,3,], Gal Kaplun[1,4], Yamini Bansal[1,4], Tristan Yang[1], Boaz Barak[1] and Ilya Sutskever[2]**

[1] Harvard University, United States of America
[2] OpenAI, United States of America
E-mail: preetum@cs.harvard.edu

Received 26 October 2021
Accepted for publication 9 November 2021
Published 29 December 2021

Online at stacks.iop.org/JSTAT/2021/124003
https://doi.org/10.1088/1742-5468/ac3a74

Abstract. We show that a variety of modern deep learning tasks exhibit a 'double-descent' phenomenon where, as we increase model size, performance first gets *worse* and then gets better. Moreover, we show that double descent occurs not just as a function of model size, but also as a function of the number of training epochs. We unify the above phenomena by defining a new complexity measure we call the *effective model complexity* and conjecture a generalized double descent with respect to this measure. Furthermore, our notion of model complexity allows us to identify certain regimes where increasing (even quadrupling) the number of train samples actually *hurts* test performance.

Keywords: deep learning, machine learning, statistical inference

J. Stat. Mech. (2021) 124003

*This article is an updated version of: Nakkiran P, Kaplun G, Bansal Y, Yang T, Barak B and Sutskever I 2020 Deep double descent: where bigger models and more data hurt *Int. Conf. Learning Representations*.
**Author to whom any correspondence should be addressed.
[3]Work performed in part while Preetum Nakkiran was interning at OpenAI, with Ilya Sutskever. We especially thank Mikhail Belkin and Christopher Olah for helpful discussions throughout this work.
[4]These authors contributed equally to this work.

Contents

1. Introduction 3
2. Our results 4
3. Related work 6
4. Experimental setup 7
5. Model-wise double descent 8
6. Epoch-wise double descent 9
7. Sample-wise non-monotonicity 11
8. Conclusion and discussion 12
Acknowledgments 15
Appendix A. Summary table of experimental results 16
Appendix B. Experimental details 16
B.1. Models 17
B.2. Image classification: experimental setup 17
B.3. Neural machine translation: experimental setup 18
B.4. Per-section experimental details 19
Appendix C. Extended discussion of related work 19
Appendix D. Random features: a case study 20
Appendix E. Appendix: additional experiments 23
E.1. Epoch-wise double descent: additional results 23
E.2. Model-wise double descent: additional results 23
E.2.1. Clean settings with model-wise double descent 23
E.2.2. Weight decay 27
E.2.3. Early stopping does not exhibit double descent 30
E.2.4. Training procedure 30
E.3. Ensembling 30
References 31

J. Stat. Mech. (2021) 124003

1. Introduction

The *bias-variance trade-off* is a fundamental concept in classical statistical learning theory (e.g. Hastie *et al* 2005). The idea is that models of higher complexity have lower bias but higher variance. According to this theory, once model complexity passes a certain threshold, models 'overfit' with the variance term dominating the test error, and hence from this point onward, increasing model complexity will only *decrease* performance (i.e. increase test error). Hence conventional wisdom in classical statistics is that, once we pass a certain threshold, *'larger models are worse'*.

However, modern neural networks exhibit no such phenomenon. Such networks have millions of parameters, more than enough to fit even random labels (Zhang *et al* 2016), and yet they perform much better on many tasks than smaller models. Indeed, conventional wisdom among practitioners is that '*larger models are better*' (Krizhevsky *et al* 2012, Huang *et al* 2018, Szegedy *et al* 2015, Radford *et al* 2019). The effect of training time on test performance is also up for debate. In some settings, 'early stopping' improves test performance, while in other settings training neural networks to zero training error only improves performance. Finally, if there is one thing both classical statisticians and deep learning practitioners agree on is *'more data is always better'*.

In this paper, we present empirical evidence that both reconcile and challenge some of the above 'conventional wisdoms'. We show that many deep learning settings have two different regimes. In the *under-parameterized* regime, where the model complexity is small compared to the number of samples, the test error as a function of model complexity follows the U-like behavior predicted by the classical bias/variance tradeoff. However, once model complexity is sufficiently large to *interpolate*, i.e. achieve (close to) zero training error, then increasing complexity only *decreases* test error, following the modern intuition of 'bigger models are better'. Similar behavior was previously observed in Opper (1995), (2001), Advani and Saxe (2017), Spigler *et al* (2018), and Geiger *et al* (2019b). This phenomenon was first postulated in generality by Belkin *et al* (2018) who named it 'double descent', and demonstrated it for decision trees, random features, and two-layer neural networks with ℓ_2 loss, on a variety of learning tasks including MNIST and CIFAR-10.

Main contributions. We show that double descent is a robust phenomenon that occurs in a variety of tasks, architectures, and optimization methods (see figure 1 and section 5; our experiments are summarized in the appendix A table). Moreover, we propose a much more general notion of 'double descent' that goes beyond varying the number of parameters. We define the *effective model complexity* (EMC) of a training procedure as the maximum number of samples on which it can achieve close to zero training error. The EMC depends not just on the data distribution and the architecture of the classifier but also on the training procedure—and in particular increasing training time will increase the EMC.

We hypothesize that for many natural models and learning algorithms, double descent occurs as a function of the EMC. Indeed we observe 'epoch-wise double descent' when we keep the model fixed and increase the training time, with performance following a classical U-like curve in the underfitting stage (when the EMC is smaller than the number of samples) and then improving with training time once the EMC is

J. Stat. Mech. (2021) 124003

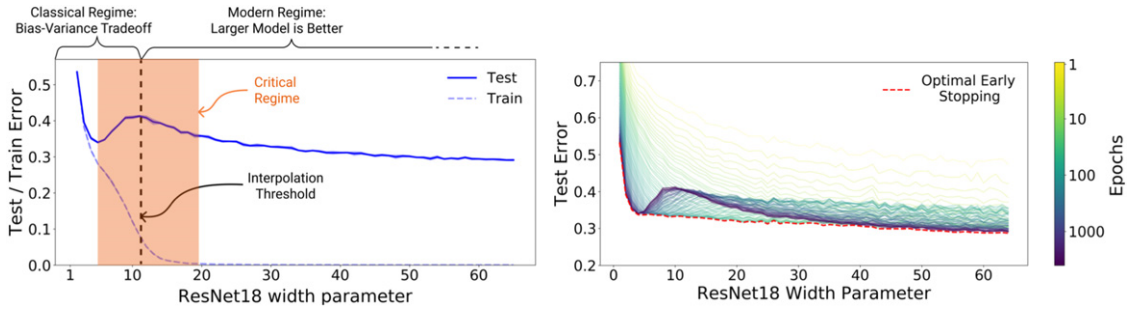

Figure 1. (Left) Train and test error as a function of model size, for ResNet18s of varying width on CIFAR-10 with 15% label noise. (Right) Test error, shown for varying train epochs. All models trained using Adam for 4K epochs. The largest model (width 64) corresponds to standard ResNet18.

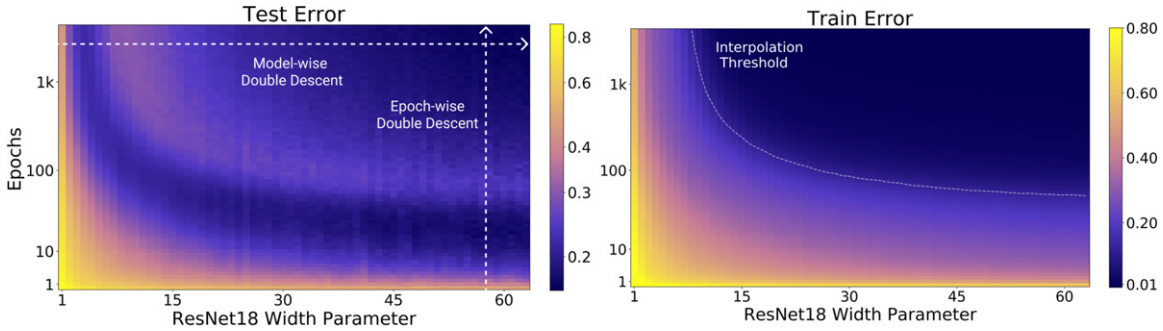

Figure 2. (Left) Test error as a function of model size and train epochs. The horizontal line corresponds to model-wise double descent—varying model size while training for as long as possible. The vertical line corresponds to epoch-wise double descent, with test error undergoing double-descent as train time increases. (Right) Train error of the corresponding models. All models are Resnet18s trained on CIFAR-10 with 15% label noise, data-augmentation, and Adam for up to 4K epochs.

sufficiently larger than the number of samples (see figure 2). As a corollary, early stopping only helps in the relatively narrow parameter regime of critically parameterized models.

Sample non-monotonicity. Finally, our results shed light on test performance as a function of the number of train samples. Since the test error peaks around the point where EMC matches the number of samples (the transition from the under- to over-parameterization), increasing the number of samples has the effect of shifting this peak to the right. While in most settings increasing the number of samples decreases error, this shifting effect can sometimes result in a setting where *more data is worse*! For example, figure 3 demonstrates cases in which increasing the number of samples by a factor of 4.5 results in worse test performance.

J. Stat. Mech. (2021) 124003

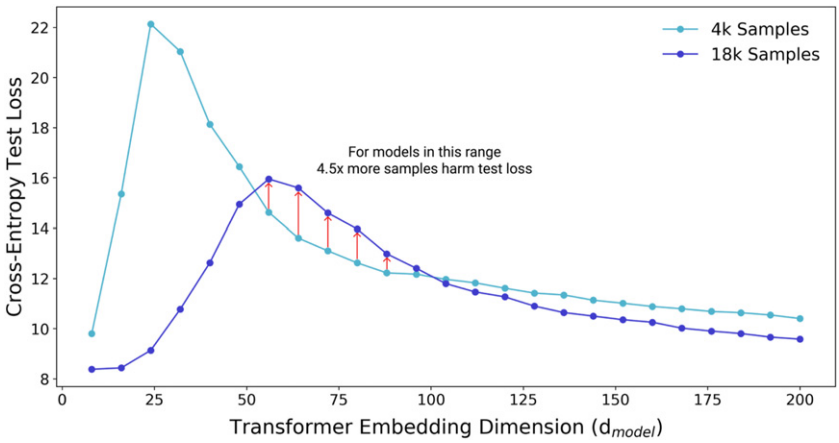

Figure 3. Test loss (per-token perplexity) as a function of transformer model size (embedding dimension d_{model}) on language translation (IWSLT'14 German-to-English). The curve for 18k samples is generally lower than the one for 4k samples, but also shifted to the right, since fitting 18k samples requires a larger model. Thus, for some models, the performance for 18k samples is *worse* than for 4k samples.

2. Our results

To state our hypothesis more precisely, we define the notion of EMC. We define a *training procedure* $\mathcal{T}$ to be any procedure that takes as input a set $S = \{(x_1, y_1), \ldots, (x_n, y_n)\}$ of labeled training samples and outputs a classifier $\mathcal{T}(S)$ mapping data to labels. We define the EMC of $\mathcal{T}$ (w.r.t. distribution $\mathcal{D}$) to be the maximum number of samples n on which $\mathcal{T}$ achieves on average ≈ 0 *training error*.

Definition 2.1 (Effective model complexity). The EMC of a training procedure $\mathcal{T}$, with respect to distribution $\mathcal{D}$ and parameter $\epsilon > 0$, is defined as:

$$\text{EMC}_{\mathcal{D},\epsilon}(\mathcal{T}) := \max\{n | \mathbb{E}_{S\sim\mathcal{D}^n}[\text{Error}_S(\mathcal{T}(S))] \leqslant \epsilon\}$$

where $\text{Error}_S(M)$ is the mean error of model M on train samples S.

Our main hypothesis can be informally stated as follows:

Hypothesis 1 (Generalized double descent hypothesis, informal). For any natural data distribution $\mathcal{D}$, neural-network-based training procedure $\mathcal{T}$, and small $\epsilon > 0$, if we consider the task of predicting labels based on n samples from $\mathcal{D}$ then:

Under-parameterized regime. If $\text{EMC}_{\mathcal{D},\epsilon}(\mathcal{T})$ is sufficiently smaller than n, any perturbation of $\mathcal{T}$ that increases its effective complexity will decrease the test error.

Over-parameterized regime. If $\text{EMC}_{\mathcal{D},\epsilon}(\mathcal{T})$ is sufficiently larger than n, any perturbation of $\mathcal{T}$ that increases its effective complexity will decrease the test error.

Critically parameterized regime. If $\text{EMC}_{\mathcal{D},\epsilon}(\mathcal{T}) \approx n$, then a perturbation of $\mathcal{T}$ that increases its effective complexity might decrease **or increase** the test error.

Hypothesis 1 is informal in several ways. We do not have a principled way to choose the parameter ϵ (and currently heuristically use $\epsilon = 0.1$). We also are yet to

J. Stat. Mech. (2021) 124003

have a formal specification for 'sufficiently smaller' and 'sufficiently larger'. Our experiments suggest that there is a *critical interval* around the *interpolation threshold* when $\mathrm{EMC}_{\mathcal{D},\epsilon}(\mathcal{T}) = n$: below and above this interval increasing complexity helps performance, while within this interval it may hurt performance. The width of the critical interval depends on both the distribution and the training procedure in ways we do not yet completely understand.

We believe hypothesis 1 sheds light on the interaction between optimization algorithms, model size, and test performance and helps reconcile some of the competing intuitions about them. The main result of this paper is an experimental validation of hypothesis 1 under a variety of settings, where we considered several natural choices of datasets, architectures, and optimization algorithms, and we changed the 'interpolation threshold' by varying the number of model parameters, the length of training, the amount of label noise in the distribution, and the number of train samples.

Model-wise double descent. In section 5, we study the test error of models of increasing size, for a fixed large number of optimization steps. We show that 'model-wise double-descent' occurs for various modern datasets (CIFAR-10, CIFAR-100, IWSLT'14 de-en, with varying amounts of label noise), model architectures (CNNs, ResNets, Transformers), optimizers (SGD, Adam), number of train samples, and training procedures (data-augmentation, and regularization). Moreover, the peak in test error systematically occurs at the interpolation threshold. In particular, we demonstrate realistic settings in which *bigger models are worse*.

Epoch-wise double descent. In section 6, we study the test error of a fixed, large architecture over the course of training. We demonstrate, in similar settings as above, a corresponding peak in test performance when models are trained just long enough to reach $\approx$0 train error. The test error of a large model first decreases (at the beginning of training), then increases (around the critical regime), then decreases once more (at the end of training)—that is, *training longer can correct overfitting.*

Sample-wise non-monotonicity. In section 7, we study the test error of a fixed model and training procedure, for varying number of train samples. Consistent with our generalized double-descent hypothesis, we observe distinct test behavior in the 'critical regime', when the number of samples is near the maximum that the model can fit. This often manifests as a long plateau region, in which taking significantly more data might not help when training to completion (as is the case for CNNs on CIFAR-10). Moreover, we show settings (Transformers on IWSLT'14 en-de), where this manifests as a peak—and for a fixed architecture and training procedure, *more data actually hurts.*

Remarks on label noise. We observe all forms of double descent most strongly in settings with label noise in the train set (as is often the case when collecting train data in the real-world). However, we also show several realistic settings with a test-error peak even without label noise: ResNets (figure 4(a)) and CNNs (figure 20) on CIFAR-100; transformers on IWSLT'14 (figure 8). Moreover, all our experiments demonstrate distinctly different test behavior in the critical regime—often manifesting as a 'plateau' in the test error in the noiseless case which develops into a peak with added label noise. See section 8 for further discussion.

J. Stat. Mech. (2021) 124003

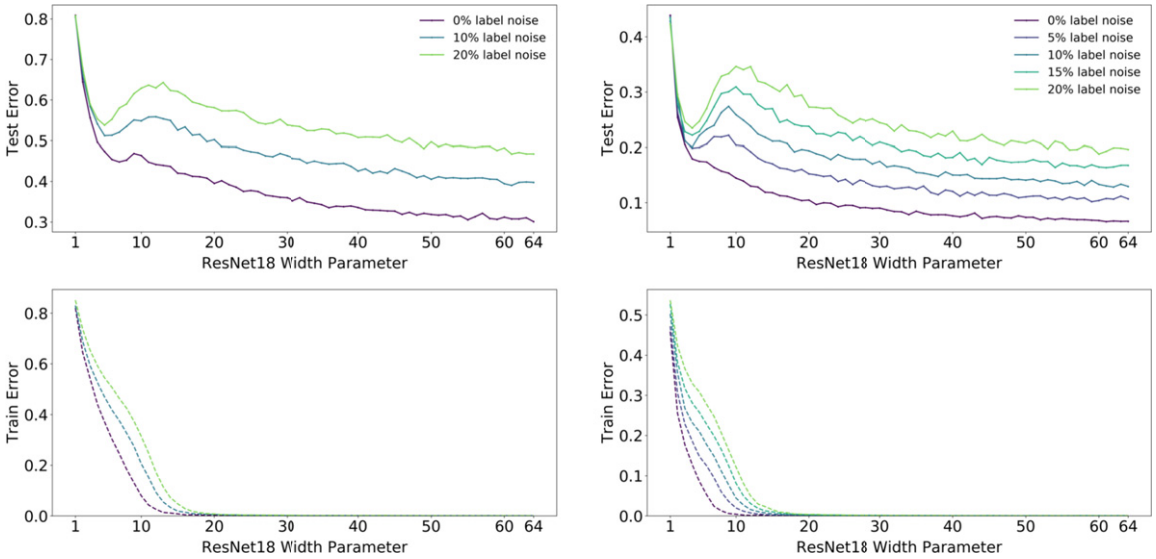

(a) **CIFAR-100.** There is a peak in test error even with no label noise.

(b) **CIFAR-10.** There is a "plateau" in test error around the interpolation point with no label noise, which develops into a peak for added label noise.

Figure 4. Model-wise double descent for ResNet18s. Trained on CIFAR-100 and CIFAR-10, with varying label noise. Optimized using Adam with LR 0.0001 for 4K epochs, and data-augmentation.

3. Related work

Model-wise double descent was first proposed as a general phenomenon by Belkin *et al* (2018). Similar behavior had been observed in Opper (1995), (2001), Advani and Saxe (2017), Spigler *et al* (2018), and Geiger *et al* (2019b). Subsequently, there has been a large body of work studying the double descent phenomenon. A growing list of papers that theoretically analyze it in the tractable setting of linear least squares regression includes Belkin *et al* (2019), Hastie *et al* (2019), Bartlett *et al* (2019), Muthukumar *et al* (2019), Bibas *et al* (2019), Mitra (2019), Mei and Montanari (2019). Moreover, Geiger *et al* (2019a) provide preliminary results for model-wise double descent in convolutional networks trained on CIFAR-10. Our work differs from the above papers in two crucial aspects: first, we extend the idea of double-descent beyond the number of parameters to incorporate the training procedure under a unified notion of 'EMC', leading to novel insights like epoch-wise double descent and sample non-monotonicity. The notion that increasing train time corresponds to increasing complexity was also presented in Nakkiran *et al* (2019). Second, we provide an extensive and rigorous demonstration of double-descent for modern practices spanning a variety of architectures, datasets optimization procedures. An extended discussion of the related work is provided in appendix C.

J. Stat. Mech. (2021) 124003

4. Experimental setup

We briefly describe the experimental setup here; full details are in appendix B.[5] We consider three families of architectures: ResNets, standard CNNs, and transformers. **ResNets:** we parameterize a family of ResNet18s (He *et al* 2016) by scaling the width (number of filters) of convolutional layers. Specifically, we use layer widths $[k, 2k, 4k, 8k]$ for varying k. The standard ResNet18 corresponds to $k = 64$. **Standard CNNs:** we consider a simple family of five-layer CNNs, with four convolutional layers of widths $[k, 2k, 4k, 8k]$ for varying k, and a fully-connected layer. For context, the CNN with width $k = 64$, can reach over 90% test accuracy on CIFAR-10 with data-augmentation. **Transformers:** we consider the 6 layer encoder-decoder from Vaswani *et al* (2017), as implemented by Ott *et al* (2019). We scale the size of the network by modifying the embedding dimension d_{model}, and setting the width of the fully-connected layers proportionally ($d_{\text{ff}} = 4 \cdot d_{\text{model}}$). For ResNets and CNNs, we train with cross-entropy loss, and the following optimizers: (1) Adam with learning-rate 0.0001 for 4K epochs; (2) SGD with learning rate $\propto \frac{1}{\sqrt{T}}$ for 500 K gradient steps. We train Transformers for 80 K gradient steps, with 10% label smoothing and no drop-out.

Label noise. In our experiments, label noise of probability p refers to training on a samples which have the correct label with probability $(1 - p)$, and a uniformly random incorrect label otherwise (label noise is sampled only once and not per epoch). Figure 1 plots test error on the noisy distribution, while the remaining figures plot test error with respect to the clean distribution (the two curves are just linear rescaling of one another).

5. Model-wise double descent

In this section, we study the test error of models of increasing size, when training to completion (for a fixed large number of optimization steps). We demonstrate model-wise double descent across different architectures, datasets, optimizers, and training procedures. The critical region exhibits distinctly different test behavior around the interpolation point and there is often a peak in test error that becomes more prominent in settings with label noise.

For the experiments in this section (figures 4–8), notice that all modifications which increase the interpolation threshold (such as adding label noise, using data augmentation, and increasing the number of train samples) also correspondingly shift the peak in test error towards larger models. Additional plots showing the early-stopping behavior of these models, and additional experiments showing double descent in settings with no label noise (e.g. figure 19) are in appendix E.2. We also observed model-wise double descent for adversarial training, with a prominent robust test error peak even in settings without label noise. See figure 26 in appendix E.2.

Discussion. Fully understanding the mechanisms behind model-wise double descent in deep neural networks remains an important open question. However, an analog of

[5] The raw data from our experiments are available at: https://gitlab.com/harvard-machine-learning/double-descent/tree/master.

J. Stat. Mech. (2021) 124003

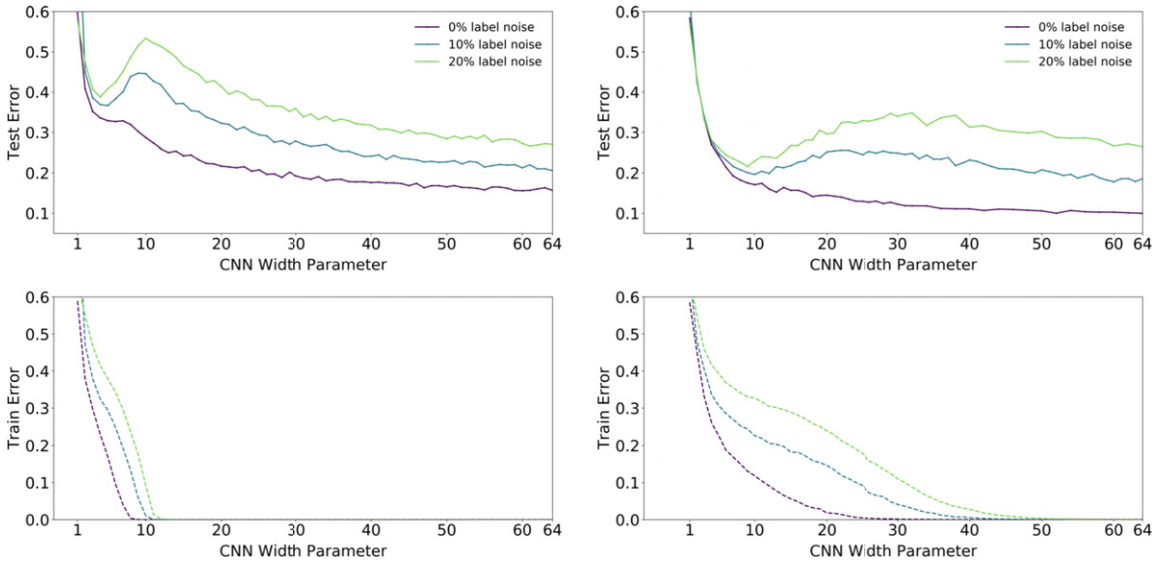

(a) Without data augmentation.

(b) With data augmentation.

Figure 5. Effect of data augmentation. Five-layer CNNs on CIFAR10, with and without data-augmentation. Data-augmentation shifts the interpolation threshold to the right, shifting the test error peak accordingly. Optimized using SGD for 500K steps. See figure 27 for larger models.

model-wise double descent occurs even for linear models. A recent stream of theoretical works analyzes this setting (Bartlett *et al* 2019, Muthukumar *et al* 2019, Belkin *et al* 2019, Mei and Montanari 2019, Hastie *et al* 2019). We believe similar mechanisms may be at work in deep neural networks.

Informally, our intuition is that for model-sizes at the interpolation threshold, there is effectively only one model that fits the train data and this interpolating model is very sensitive to noise in the train set and/or model mis-specification. That is, since the model is just barely able to fit the train data, forcing it to fit even slightly-noisy or mis-specified labels will destroy its global structure, and result in high test error. (See figure 28 in the appendix for an experiment demonstrating this noise sensitivity, by showing that ensembling helps significantly in the critically-parameterized regime.) However for over-parameterized models, there are many interpolating models that fit the train set, and SGD is able to find one that 'memorizes' (or 'absorbs') the noise while still performing well on the distribution.

The above intuition is theoretically justified for linear models. In general, this situation manifests even without label noise for linear models (Mei and Montanari 2019), and occurs whenever there is *model mis-specification* between the structure of the true distribution and the model family. We believe this intuition extends to deep learning as well, and it is consistent with our experiments.

J. Stat. Mech. (2021) 124003

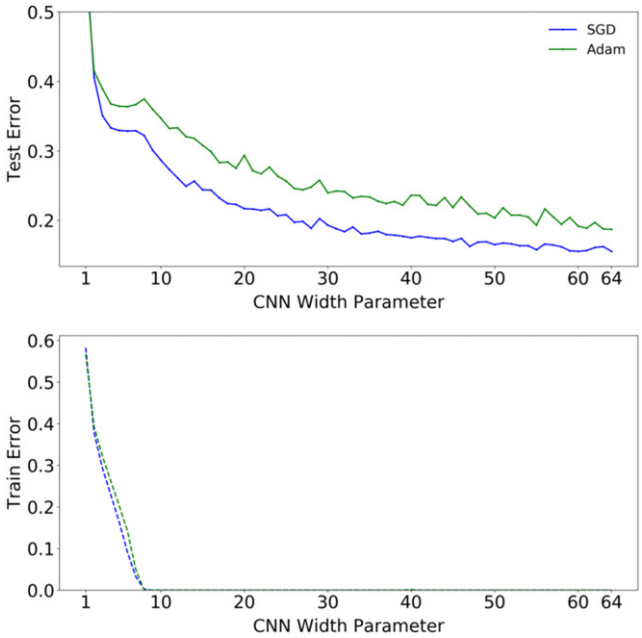

Figure 6. SGD vs Adam. Five-layer CNNs on CIFAR-10 with no label noise, and no data augmentation. Optimized using SGD for 500K gradient steps, and Adam for 4K epochs.

6. Epoch-wise double descent

In this section, we demonstrate a novel form of double-descent with respect to training epochs, which is consistent with our unified view of EMC and the generalized double descent hypothesis. Increasing the train time increases the EMC—and thus a sufficiently large model transitions from under- to over-parameterized over the course of training.

As illustrated in figure 9, sufficiently large models can undergo a 'double descent' behavior where test error first decreases then increases near the interpolation threshold, and then decreases again. In contrast, for 'medium sized' models, for which training to completion will only barely reach ≈ 0 error, the test error as a function of training time will follow a classical U-like curve where it is better to stop early. Models that are too small to reach the approximation threshold will remain in the 'under parameterized' regime where increasing train time monotonically decreases test error. Our experiments (figure 10) show that many settings of dataset and architecture exhibit epoch-wise double descent, in the presence of label noise. Further, this phenomenon is robust across optimizer variations and learning rate schedules (see additional experiments in appendix E.1). As in model-wise double descent, the test error peak is accentuated with label noise.

Conventional wisdom suggests that training is split into two phases: (1) in the first phase, the network learns a function with a small generalization gap (2) in the second

J. Stat. Mech. (2021) 124003

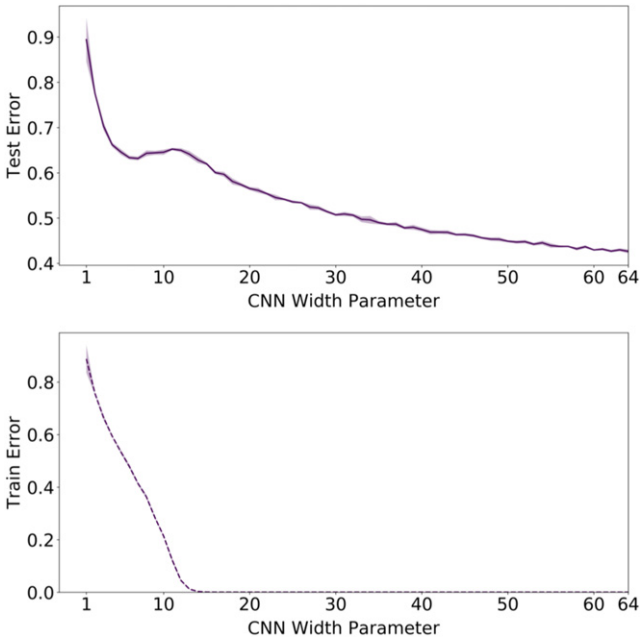

Figure 7. Noiseless settings. Five-layer CNNs on CIFAR-100 with no label noise; note the peak in test error. Trained with SGD and no data augmentation. See figure 20 for the early-stopping behavior of these models.

phase, the network starts to over-fit the data leading to an increase in test error. Our experiments suggest that this is not the complete picture—in some regimes, the test error decreases again and may achieve a lower value at the end of training as compared to the first minimum (see figure 10 for 10% label noise).

7. Sample-wise non-monotonicity

In this section, we investigate the effect of varying the number of train samples, for a fixed model and training procedure. Previously, in model-wise and epoch-wise double descent, we explored behavior in the critical regime, where $\mathrm{EMC}_{\mathcal{D},\epsilon}(\mathcal{T}) \approx n$, by varying the EMC. Here, we explore the critical regime by varying the number of train samples n. By increasing n, the same training procedure $\mathcal{T}$ can switch from being effectively over-parameterized to effectively under-parameterized.

We show that increasing the number of samples has two different effects on the test error vs model complexity graph. On the one hand, (as expected) increasing the number of samples shrinks the area under the curve. On the other hand, increasing the number of samples also has the effect of 'shifting the curve to the right' and increasing the model complexity at which test error peaks.

These twin effects are shown in figure 11(a). Note that there is a range of model sizes where the effects 'cancel out'—and having 4× more train samples does not help test performance when training to completion. Outside the critically-parameterized regime, for sufficiently under- or over-parameterized models, having more samples helps. This

J. Stat. Mech. (2021) 124003

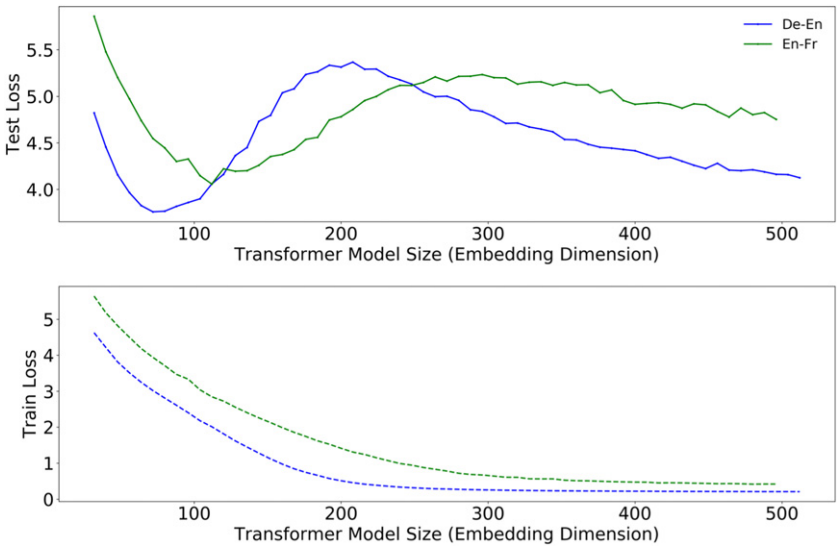

Figure 8. Transformers on language translation tasks: multi-head-attention encoder-decoder transformer model trained for 80k gradient steps with labeled smoothed cross-entropy loss on IWSLT'14 German-to-English (160K sentences) and WMT'14 English-to-French (subsampled to 200K sentences) dataset. Test loss is measured as per-token perplexity.

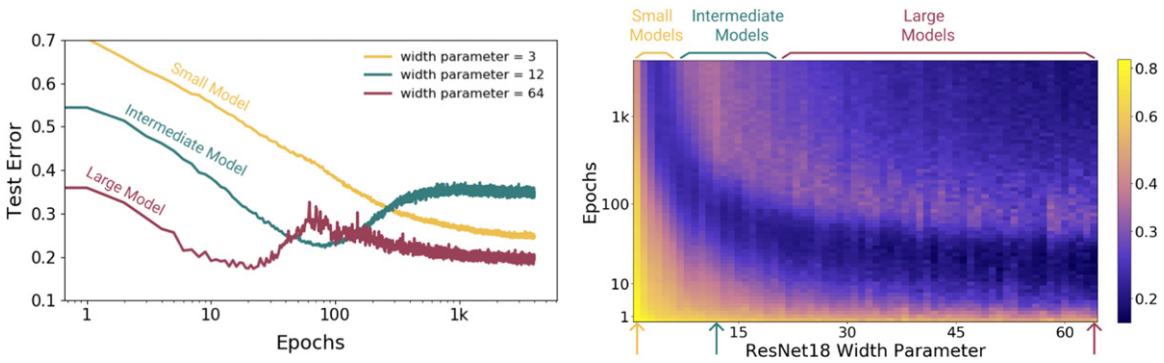

Figure 9. (Left) Training dynamics for models in three regimes. Models are ResNet18s on CIFAR10 with 20% label noise, trained using Adam with learning rate 0.0001, and data augmentation. (Right) Test error over (model size × Epochs). Three slices of this plot are shown on the left.

phenomenon is corroborated in figure 12, which shows test error as a function of both model and sample size, in the same setting as figure 11(a).

In some settings, these two effects combine to yield a regime of model sizes where more data actually hurts test performance as in figure 3 (see also figure 11(b)). Note that this phenomenon is not unique to DNNs: more data can hurt even for linear models (see appendix D).

J. Stat. Mech. (2021) 124003

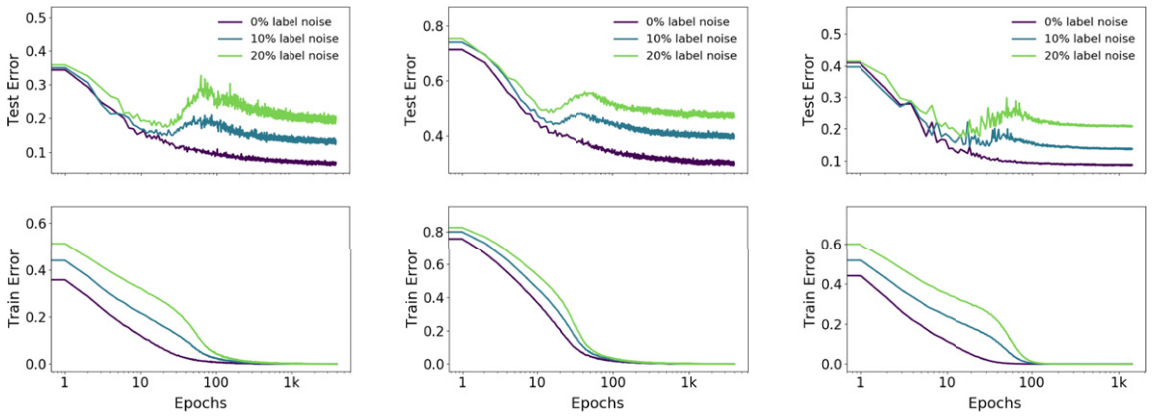

(a) ResNet18 on CIFAR10. (b) ResNet18 on CIFAR100. (c) 5-layer CNN on CIFAR 10.

Figure 10. Epoch-wise double descent for ResNet18 and CNN (width = 128). ResNets trained using Adam with learning rate 0.0001, and CNNs trained with SGD with inverse-squareroot learning rate.

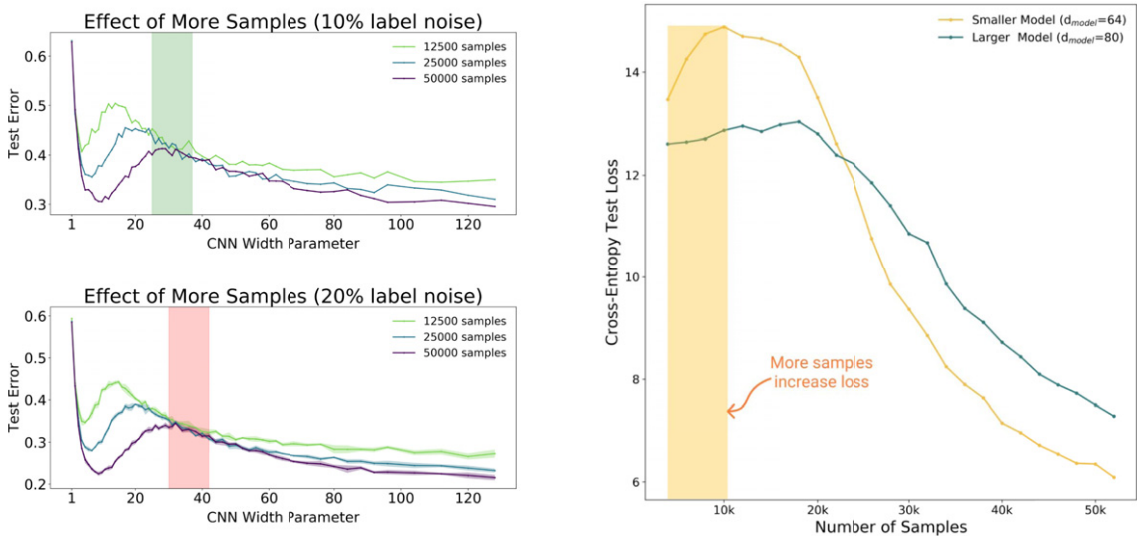

(a) Model-wise double descent for 5-layer CNNs on CIFAR-10, for varying dataset sizes. **Top:** There is a range of model sizes (shaded green) where training on 2× more samples does not improve test error. **Bottom:** There is a range of model sizes (shaded red) where training on 4× more samples does not improve test error.

(b) **Sample-wise non-monotonicity.** Test loss (per-word perplexity) as a function of number of train samples, for two transformer models trained to completion on IWSLT'14. For both model sizes, there is a regime where more samples hurt performance. Compare to Figure 3, of model-wise double-descent in the identical setting.

Figure 11. Sample-wise non-monotonicity.

J. Stat. Mech. (2021) 124003

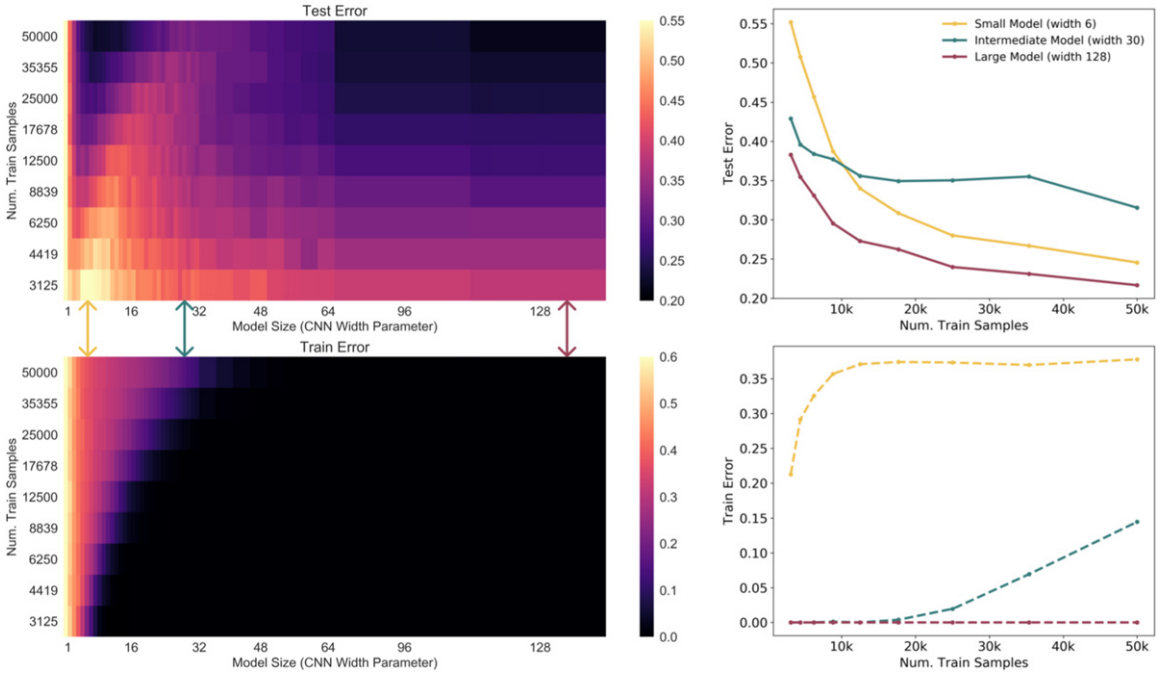

Figure 12. (Left) Test error as a function of model size and number of train samples, for five-layer CNNs on CIFAR-10 + 20% noise. Note the ridge of high test error again lies along the interpolation threshold. (Right) Three slices of the left plot, showing the effect of more data for models of different sizes. Note that, when training to completion, more data helps for small and large models, but does not help for near-critically-parameterized models (green).

8. Conclusion and discussion

We introduce a generalized double descent hypothesis: models and training procedures exhibit atypical behavior when their EMC is comparable to the number of train samples. We provide extensive evidence for our hypothesis in modern deep learning settings, and show that it is robust to choices of dataset, architecture, and training procedures. In particular, we demonstrate 'model-wise double descent' for modern deep networks and characterize the regime where bigger models can perform worse. We also demonstrate 'epoch-wise double descent', which, to the best of our knowledge, has not been previously proposed. Finally, we show that the double descent phenomenon can lead to a regime where training on more data leads to worse test performance. Preliminary results suggest that double descent also holds as we vary the amount of regularization for a fixed model (see figure 22).

We also believe our characterization of the critical regime provides a useful way of thinking for practitioners—if a model and training procedure are just barely able to fit the train set, then small changes to the model or training procedure may yield unexpected behavior (e.g. making the model slightly larger or smaller, changing regularization, etc, may hurt test performance).

J. Stat. Mech. (2021) 124003

Early stopping. We note that many of the phenomena that we highlight often do not occur with optimal early-stopping. However, this is consistent with our generalized double descent hypothesis: if early stopping prevents models from reaching 0 train error then we would not expect to see double-descent, since the EMC does not reach the number of train samples. Further, we show at least one setting where model-wise double descent can still occur even with optimal early stopping (ResNets on CIFAR-100 with no label noise, see figure 19). We have not observed settings where more data hurts when optimal early-stopping is used. However, we are not aware of reasons which preclude this from occurring. We leave fully understanding the optimal early stopping behavior of double descent as an important open question for future work.

Label noise. In our experiments, we observe double descent most strongly in settings with label noise. However, we believe this effect is not fundamentally about label noise, but rather about *model mis-specification*. For example, consider a setting where the label noise is not truly random, but rather pseudorandom (with respect to the family of classifiers being trained). In this setting, the performance of the Bayes optimal classifier would not change (since the pseudorandom noise is deterministic, and invertible), but we would observe an identical double descent as with truly random label noise. Thus, we view adding label noise as merely a proxy for making distributions 'harder'—i.e. increasing the amount of model mis-specification.

Other notions of model complexity. Our notion of EMC is related to classical complexity notions such as Rademacher complexity, but differs in several crucial ways: (1) EMC depends on the *true labels* of the data distribution, and (2) EMC depends on the training procedure, not just the model architecture.

Other notions of model complexity which do not incorporate features (1) and (2) would not suffice to characterize the location of the double-descent peak. Rademacher complexity, for example, is determined by the ability of a model architecture to fit a randomly-labeled train set. But Rademacher complexity and VC dimension are both insufficient to determine the model-wise double descent peak location, since they do not depend on the distribution of labels—and our experiments show that adding label noise shifts the location of the peak.

Moreover, both Rademacher complexity and VC dimension depend only on the model family and data distribution, and not on the training procedure used to find models. Thus, they are not capable of capturing train-time double-descent effects, such as 'epoch-wise' double descent, and the effect of data-augmentation on the peak location.

Acknowledgments

We thank Mikhail Belkin for extremely useful discussions in the early stages of this work. We thank Christopher Olah for suggesting the Model Size × Epoch visualization, which led to the investigation of epoch-wise double descent, as well as for useful discussion and feedback. We also thank Alec Radford, Jacob Steinhardt, and Vaishaal Shankar for helpful discussion and suggestions. P N thanks OpenAI, the Simons

Institute, and the Harvard Theory Group for a research environment that enabled this kind of work. We thank Dimitris Kalimeris, Benjamin L Edelman, and Sharon Qian, and Aditya Ramesh for comments on an early draft of this work. This work supported in part by NSF Grant CAREER CCF 1452961, BSF Grant 2014389, NSF USICCS proposal 1540428, a Google Research award, a Facebook research award, a Simons Investigator Award, a Simons Investigator Fellowship, and NSF Awards CCF 1715187, CCF 1565264, CCF 1301976, IIS 1409097, and CNS 1618026. Y B would like to thank the MIT-IBM Watson AI Lab for contributing computational resources for experiments.

Appendix A. Summary table of experimental results

Dataset	Architecture	Opt.	Aug.	% Noise	Double-descent		Figure(s)
					Model	Epoch	
CIFAR 10	CNN	SGD	✓	0	✗	✗	5 and 27
			✓	10	✓	✓	5, 27 and 6
			✓	20	✓	✓	5 and 27
				0	✗	✗	5 and 25
				10	✓	✓	5
				20	✓	✓	5
		SGD + w.d.	✓	20	✓	✓	21
		Adam		0	✓	—	25
	ResNet	Adam	✓	0	✗	✗	4 and 10
			✓	5	✓	—	4
			✓	10	✓	✓	4 and 10
			✓	15	✓	✓	4 and 2
			✓	20	✓	✓	4, 9 and 10
		Various	✓	20	—	✓	16–18
(Subsampled)	CNN	SGD	✓	10	✓	—	11(a)
		SGD	✓	20	✓	—	11(a) and 12
(Adversarial)	ResNet	SGD		0	Robust err.	—	26
CIFAR 100	ResNet	Adam	✓	0	✓	✗	4, 19 and 10
			✓	10	✓	✓	4 and 10
			✓	20	✓	✓	4 and 10
	CNN	SGD		0	✓	✗	20
IWSLT '14 de-en	Transformer	Adam		0	✓	✗	8 and 24
(Subsampled)	Transformer	Adam		0	✓	✗	11(b) and 23
WMT '14 en-fr	Transformer	Adam		0	✓	✗	8 and 24

J. Stat. Mech. (2021) 124003

Appendix B. Experimental details

B.1. Models

We use the following families of architectures. The PyTorch Paszke *et al* (2017) specification of our ResNets and CNNs are available at https://gitlab.com/harvard-machine-learning/double-descent/tree/master.

ResNets. We define a family of ResNet18s of increasing size as follows. We follow the Preactivation ResNet18 architecture of He *et al* (2016), using 4 ResNet blocks, each consisting of two BatchNorm-ReLU-convolution layers. The layer widths for the four blocks are $[k, 2k, 4k, 8k]$ for varying $k \in \mathbb{N}$ and the strides are [1, 2, 2, 2]. The standard ResNet18 corresponds to $k = 64$ convolutional channels in the first layer. The scaling of model size with k is shown in figure 13(b). Our implementation is adapted from https://github.com/kuangliu/pytorch-cifar.

Standard CNNs. We consider a simple family of five-layer CNNs, with four Conv-BatchNorm-ReLU-MaxPool layers and a fully-connected output layer. We scale the four convolutional layer widths as $[k, 2k, 4k, 8k]$. The MaxPool is [1, 2, 2, 8]. For all the convolution layers, the kernel size = 3, stride = 1 and padding = 1. This architecture is based on the 'backbone' architecture from Page (2018). For $k = 64$, this CNN has 1558 026 parameters and can reach >90% test accuracy on CIFAR-10 (Krizhevsky 2009) with data-augmentation. The scaling of model size with k is shown in figure 13(a).

Transformers. We consider the encoder-decoder transformer model from Vaswani *et al* (2017) with six layers and eight attention heads per layer, as implemented by fairseq Ott *et al* (2019). We scale the size of the network by modifying the embedding dimension (d_{model}), and scale the width of the fully-connected layers proportionally ($d_{\text{ff}} = 4d_{\text{model}}$). We train with 10% label smoothing and no drop-out, for 80 gradient steps.

B.2. Image classification: experimental setup

We describe the details of training for CNNs and ResNets below.

Loss function: unless stated otherwise, we use the cross-entropy loss for all the experiments.

Data-augmentation: in experiments where data-augmentation was used, we apply `RandomCrop(32, padding = 4)` and `RandomHorizontalFlip`. In experiments with added label noise, the label for all augmentations of a given training sample are given the same label.

Regularization: no explicit regularization like weight decay or dropout was applied unless explicitly stated.

Initialization: we use the default initialization provided by PyTorch for all the layers.

Optimization:

- **Adam:** unless specified otherwise, learning rate was set at constant to $1e-4$ and all other parameters were set to their default PyTorch values.

J. Stat. Mech. (2021) 124003

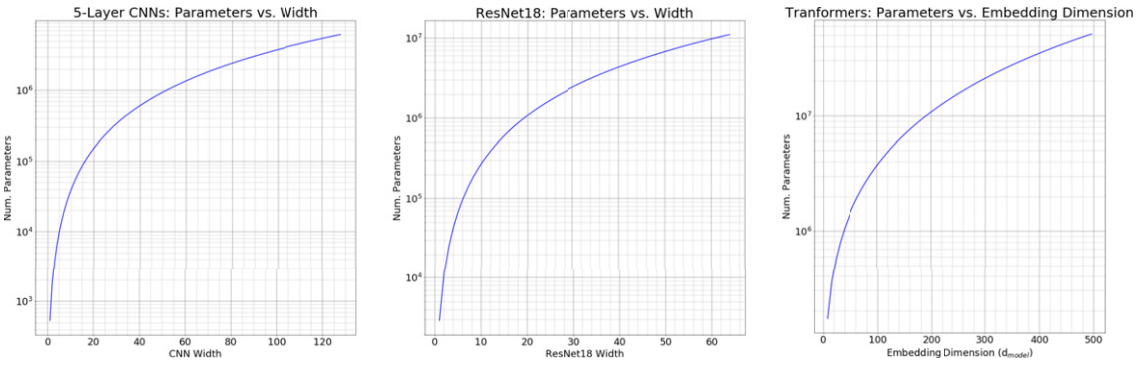

(a) 5-layer CNNs (b) ResNet18s (c) Transformers

Figure 13. Scaling of model size with our parameterization of width & embedding dimension.

- **SGD:** unless specified otherwise, learning rate schedule inverse-square root (defined below) was used with initial learning rate $\gamma_0 = 0.1$ and updates every $L = 512$ gradient steps. No momentum was used.

We found our results are robust to various other natural choices of optimizers and learning rate schedule. We used the above settings because (1) they optimize well, and (2) they do not require experiment-specific hyperparameter tuning, and allow us to use the same optimization across many experiments.

Batch size: all experiments use a batchsize of 128.

Learning rate schedule descriptions:

- **Inverse-square root (γ_0, L)**: at gradient step t, the learning rate is set to $\gamma(t) := \frac{\gamma_0}{\sqrt{1+\lfloor t/512 \rfloor}}$. We set learning-rate with respect to number of gradient steps, and not epochs, in order to allow comparison between experiments with varying train-set sizes.
- **Dynamic drop (γ_0, drop, patience)**: starts with an initial learning rate of γ_0 and drops by a factor of 'drop' if the training loss has remained constant or become worse for 'patience' number of gradient steps.

B.3. Neural machine translation: experimental setup

Here we describe the experimental setup for the neural machine translation experiments.

Training procedure. In this setting, the distribution $\mathcal{D}$ consists of triples

$$(x, y, i) \,:\, x \in V_{\text{src}}^*,\ y \in V_{\text{tgt}}^*, \quad i \in \{0, \ldots, |y|\}$$

where V_{src} and V_{tgt} are the source and target vocabularies, the string x is a sentence in the source language, y is its translation in the target language, and i is the index of the token to be predicted by the model. We assume that $i|x, y$ is distributed uniformly on $\{0, \ldots, |y|\}$.

J. Stat. Mech. (2021) 124003

A standard probabilistic model defines an autoregressive factorization of the likelihood:

$$p_M(y|x) = \prod_{i=1}^{|y|} p_M(y_i|y_{<i}, x).$$

Given a set of training samples S, we define

$$\text{Error}_S(M) = \frac{1}{|S|} \sum_{(x,y,i)\in S} -\log\, p_M(y_i|y_{<i}, x).$$

In practice, S is *not* constructed from independent samples from D, but rather by first sampling (x, y) and then including all $(x, y, 0), \ldots, (x, y, |y|)$ in S.

For training transformers, we replicate the optimization procedure specified in Vaswani *et al* (2017) section 5.3, where the learning rate schedule consists of a 'warmup' phase with linearly increasing learning rate followed by a phase with inverse square-root decay. We preprocess the data using byte pair encoding as described in Sennrich *et al* (2015). We use the implementation provided by fairseq (https://github.com/pytorch/fairseq).

Datasets. The IWSLT'14 German to English dataset contains TED Talks as described in Cettolo *et al* (2012). The WMT'14 English to French dataset is taken from http://statmt.org/wmt14/translation-task.html.

B.4. Per-section experimental details

Here we provide full details for experiments in the body, when not otherwise provided.

Introduction: experimental details figure 1: all models were trained using Adam with learning-rate 0.0001 for 4K epochs. Plotting means and standard deviations for five trials, with random network initialization.

Model-wise double descent: experimental details figure 7: plotting means and standard deviations for five trials, with random network initialization.

Sample-wise nonmonotonicity: experimental details figure 11(a): all models are trained with SGD for 500K epochs, and data-augmentation. Bottom: means and standard deviations from five trials with random initialization, and random subsampling of the train set.

Appendix C. Extended discussion of related work

Belkin *et al* (2018): this paper proposed, in very general terms, that the apparent contradiction between traditional notions of the bias-variance trade-off and empirically successful practices in deep learning can be reconciled under a double-descent curve—as model complexity increases, the test error follows the traditional 'U-shaped curve', but beyond the point of interpolation, the error starts to *decrease*. This work provides empirical evidence for the double-descent curve with fully connected networks trained on subsets of MNIST, CIFAR10, SVHN and TIMIT datasets. They use the l_2 loss for their experiments. They demonstrate that neural networks are not an aberration in this

J. Stat. Mech. (2021) 124003

regard—double-descent is a general phenomenon observed also in linear regression with random features and random forests.

Theoretical works on linear least squares regression: a variety of papers have attempted to theoretically analyze this behavior in restricted settings, particularly the case of least squares regression under various assumptions on the training data, feature spaces and regularization method.

(a) Advani and Saxe (2017), Hastie *et al* (2019) both consider the linear regression problem stated above and analyze the generalization behavior in the asymptotic limit $N, D \to \infty$ using random matrix theory. Hastie *et al* (2019) highlight that when the model is mis-specified, the minimum of training error can occur for over-parameterized models

(b) Belkin *et al* (2019) linear least squares regression for two data models, where the input data is sampled from a Gaussian and a Fourier series model for functions on a circle. They provide a finite-sample analysis for these two cases

(c) Bartlett *et al* (2019) provides generalization bounds for the minimum l_2-norm interpolant for Gaussian features

(d) Muthukumar *et al* (2019) characterize the fundamental limit of any interpolating solution in the presence of noise and provide some interesting Fourier-theoretic interpretations.

(e) Mei and Montanari (2019): this work provides asymptotic analysis for ridge regression over random features

Similar double descent behavior was investigated in Opper (1995), (2001).

Geiger *et al* (2019b) showed that deep fully connected networks trained on the MNIST dataset with hinge loss exhibit a 'jamming transition' when the number of parameters exceeds a threshold that allows training to near-zero train loss. Geiger *et al* (2019a) provide further experiments on CIFAR-10 with a convolutional network. They also highlight interesting behavior with ensembling around the critical regime, which is consistent with our informal intuitions in section 5 and our experiments in figures 28 and 29.

Advani and Saxe (2017), Geiger *et al* (2019b), (2019a) also point out that double-descent is not observed when optimal early-stopping is used.

Appendix D. Random features: a case study

In this section, for completeness sake, we show that both the model- and sample-wise double descent phenomena are not unique to deep neural networks—they exist even in the setting of random Fourier features of Rahimi and Recht (2008). This setting is equivalent to a two-layer neural network with e^{-ix} activation. The first layer is initialized with a $\mathcal{N}(0, \frac{1}{d})$ Gaussian distribution and then fixed throughout training. The width (or embedding dimension) d of the first layer parameterizes the model size. The second layer is initialized with 0s and trained with MSE loss.

J. Stat. Mech. (2021) 124003

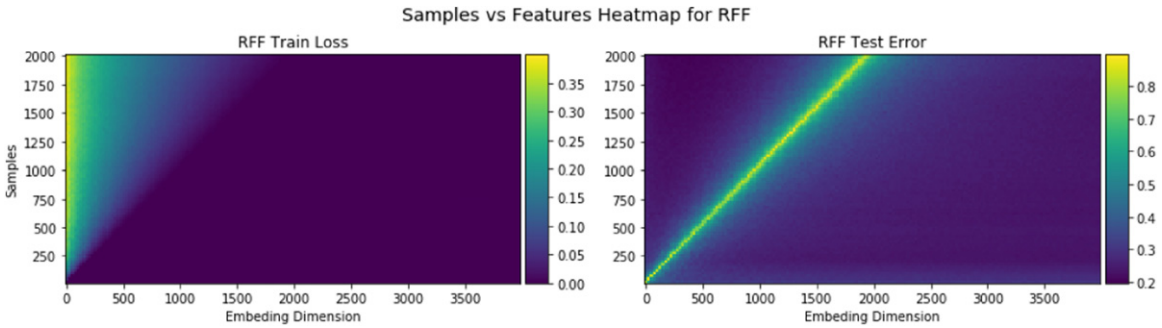

Figure 14. Random Fourier features on the Fashion MNIST dataset. The setting is equivalent to two-layer neural network with e^{-ix} activation, with randomly-initialized first layer that is fixed throughout training. The second layer is trained using gradient flow.

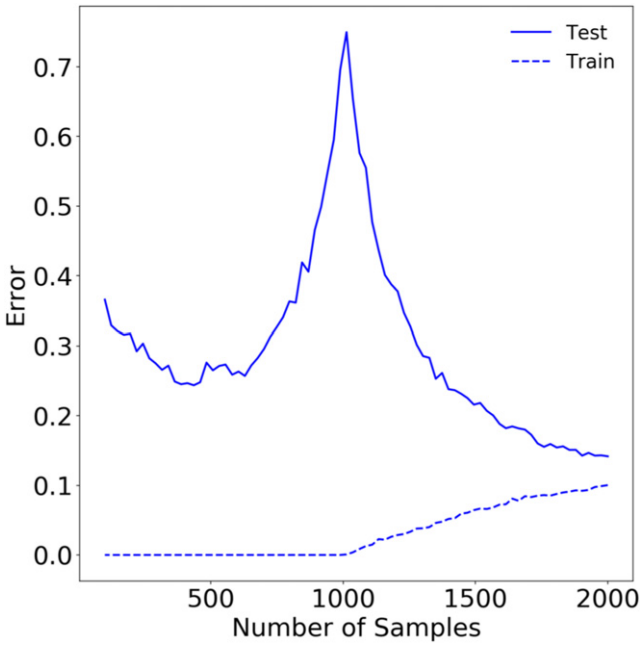

Figure 15. Sample-wise double-descent slice for random Fourier features on the Fashion MNIST dataset. In this figure the embedding dimension (number of random features) is 1000.

J. Stat. Mech. (2021) 124003

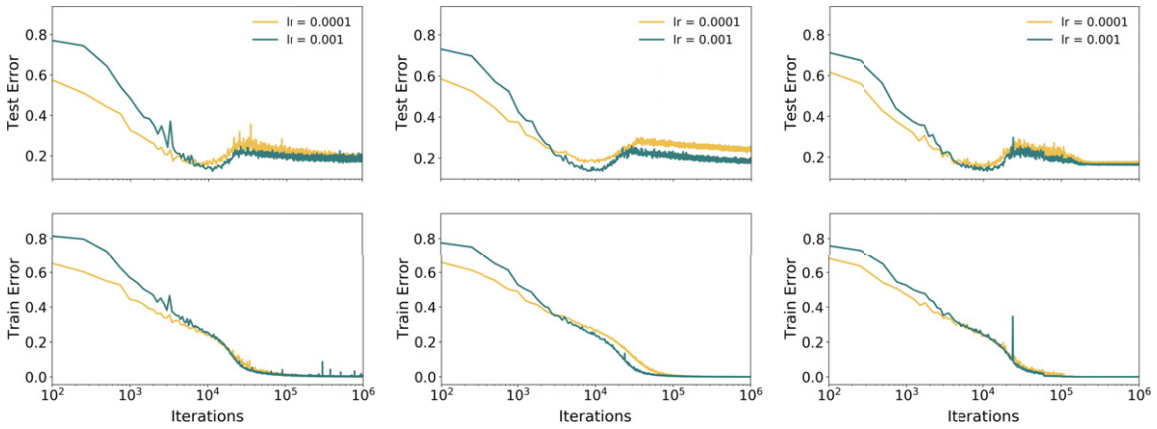

(a) Constant learning rate (b) Inverse-square root learning rate (c) Dynamic learning rate

Figure 16. Epoch-wise double descent for ResNet18 trained with Adam and multiple learning rate schedules.

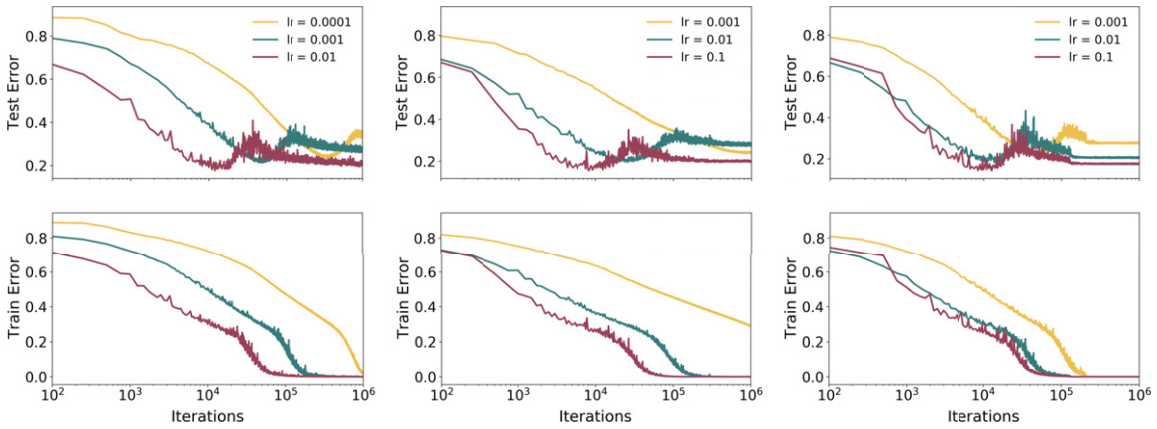

(a) Constant learning rate (b) Inverse-square root learning rate (c) Dynamic learning rate

Figure 17. Epoch-wise double descent for ResNet18 trained with SGD and multiple learning rate schedules.

J. Stat. Mech. (2021) 124003

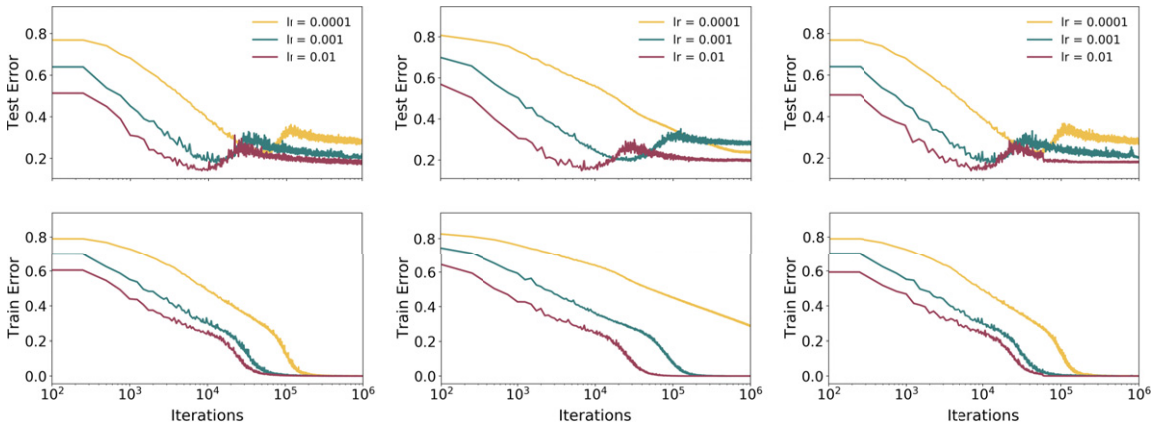

(a) Constant learning rate (b) Inverse-square root learning rate (c) Dynamic learning rate

Figure 18. Epoch-wise double descent for ResNet18 trained with SGD + momentum and multiple learning rate schedules.

Figure 14 shows the grid of test error as a function of both number of samples n and model size d. Note that in this setting EMC $= d$ (the embedding dimension). As a result, as demonstrated in the figure, the peak follows the path of $n = d$. Both model-wise and sample-wise (see figure 15) double descent phenomena are captured, by horizontally and vertically crossing the grid, respectively.

Appendix E. Appendix: additional experiments

E.1. Epoch-wise double descent: additional results

Here, we provide a rigorous evaluation of epoch-wise double descent for a variety of optimizers and learning rate schedules. We train ResNet18 on CIFAR-10 with data-augmentation and 20% label noise with three different optimizers—Adam, SGD, SGD + momentum (momentum set to 0.9) and three different learning rate schedules—constant, inverse-square root, dynamic drop for different values of initial learning rate. We observe that double-descent occurs reliably for all optimizers and learning rate schedules and the peak of the double descent curve shifts with the interpolation point (figures 16–29).

A practical recommendation resulting from epoch-wise double descent is that stopping the training when the test error starts to increase may not always be the best strategy. In some cases, the test error may decrease again after reaching a maximum, and the final value may be lower than the minimum earlier in training.

E.2. Model-wise double descent: additional results

E.2.1. Clean settings with model-wise double descent.

J. Stat. Mech. (2021) 124003

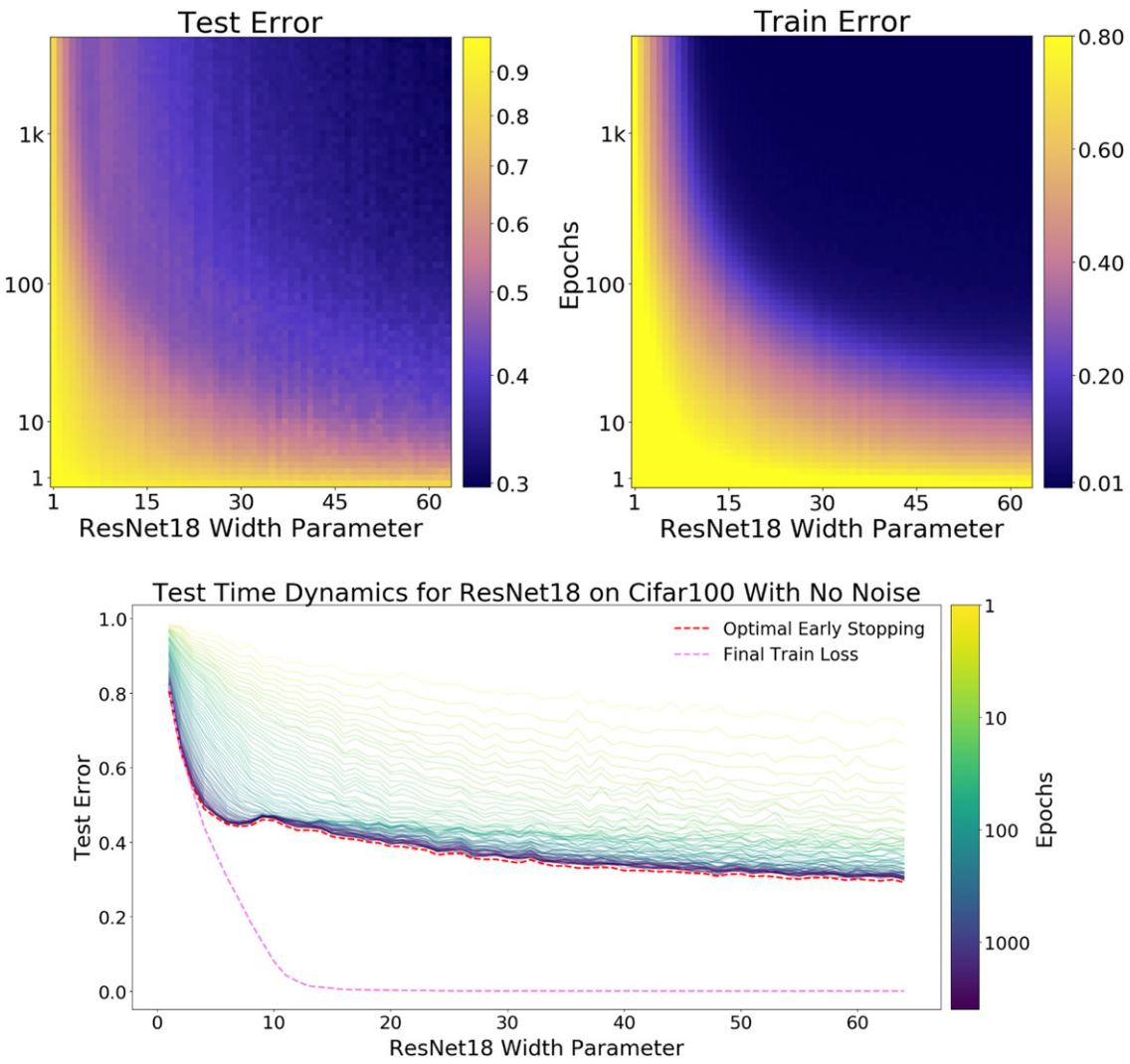

Figure 19. (Top) Train and test performance as a function of both model size and train epochs. (Bottom) Test error dynamics of the same model (ResNet18, on CIFAR-100 with no label noise, data-augmentation and Adam optimizer trained for 4k epochs with learning rate 0.0001). Note that even with optimal early stopping this setting exhibits double descent.

J. Stat. Mech. (2021) 124003

CIFAR100, Standard CNN

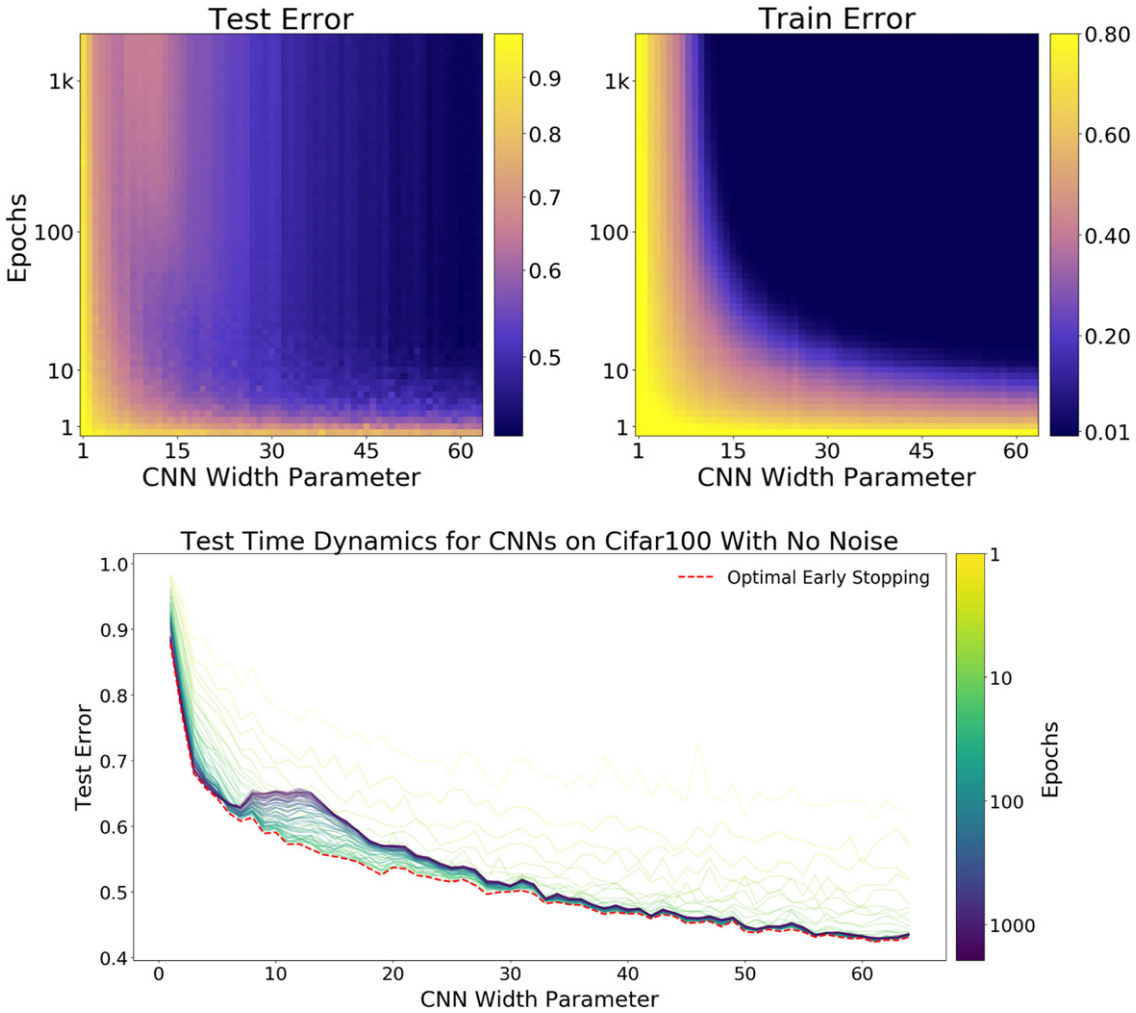

Figure 20. (Top) Train and test performance as a function of both model size and train epochs. (Bottom) Test error dynamics of the same models. Five-layer CNNs, CIFAR-100 with no label noise, no data-augmentation trained with SGD for 1×10^6 steps. Same experiment as figure 7.

J. Stat. Mech. (2021) 124003

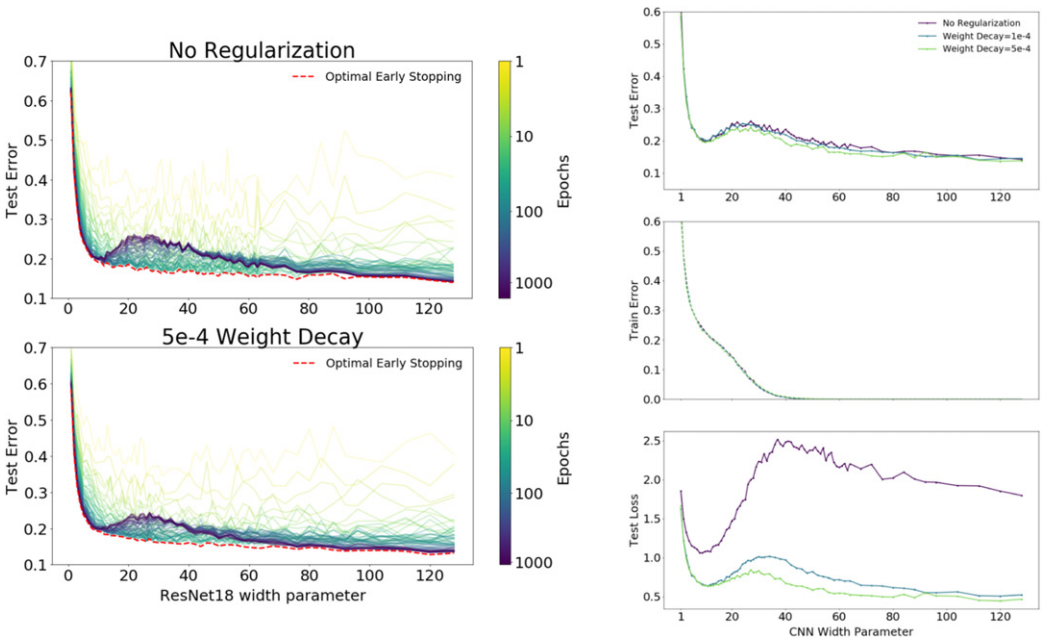

Figure 21. (Left) Test error dynamics with weight decay of 5×10^{-4} (bottom left) and without weight decay (top left). (Right) Test and train error and *test loss* for models with varying amounts of weight decay. All models are five-layer CNNs on CIFAR-10 with 10% label noise, trained with data-augmentation and SGD for 500K steps.

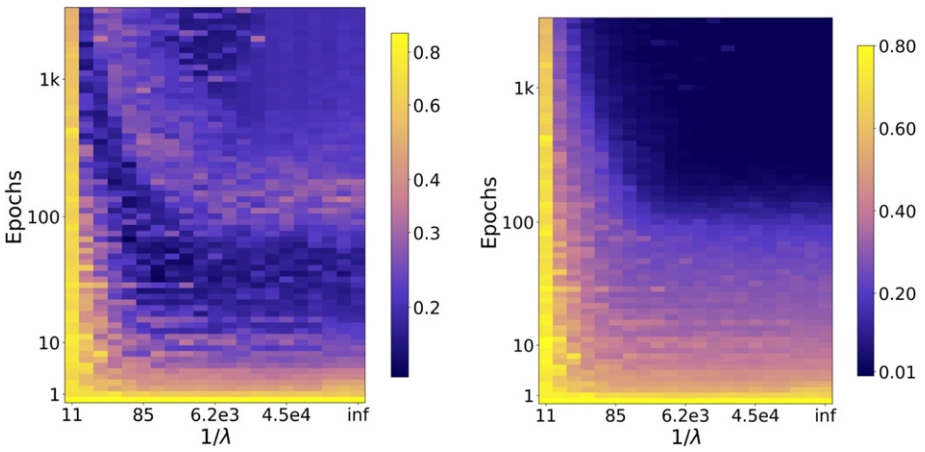

(a) Test Error (b) Train Loss

Figure 22. Generalized double descent for weight decay. We found that using the same initial learning rate for all weight decay values led to training instabilities. This resulted in some noise in the test error (weight decay × Epochs) plot shown above.

J. Stat. Mech. (2021) 124003

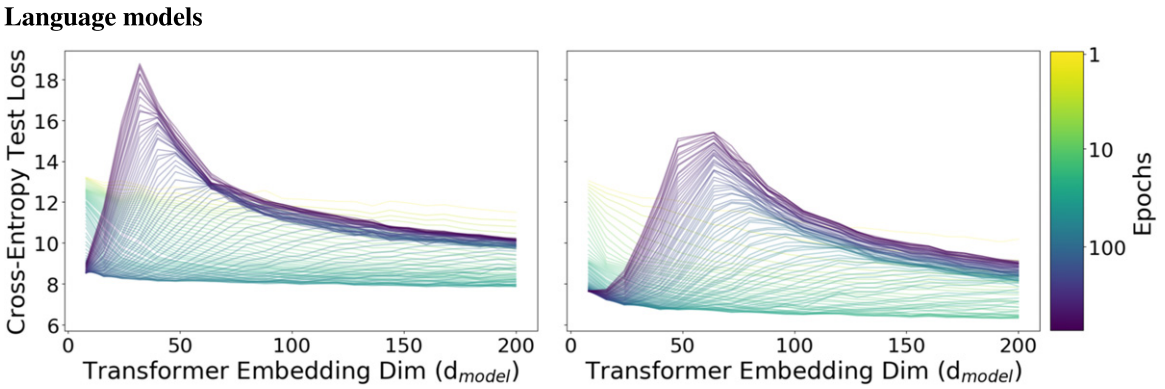

Figure 23. Model-wise test error dynamics for a subsampled IWSLT'14 dataset. (Left) 4k samples. (Right) 18k samples. Note that with optimal early-stopping, more samples is always better.

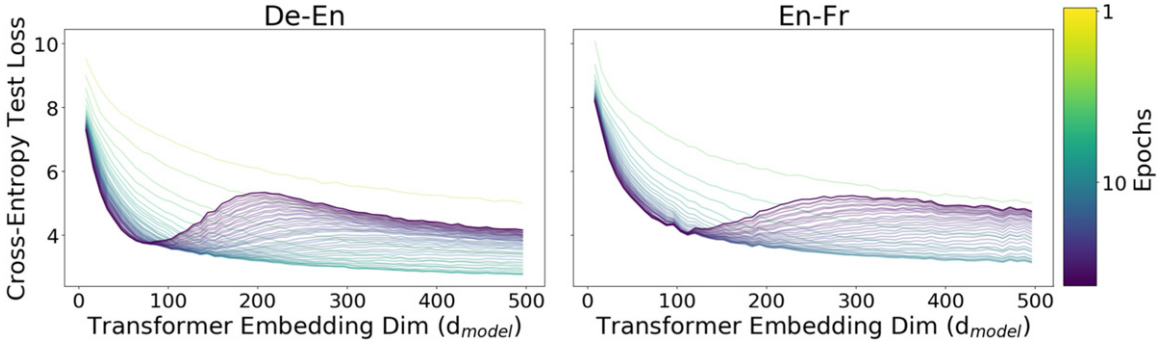

Figure 24. Model-wise test error dynamics for a IWSLT'14 de-en and subsampled WMT'14 en-fr datasets. (Left) IWSLT'14. (Right) subsampled (200k samples) WMT'14. Note that with optimal early-stopping, the test error is much lower for this task.

E.2.2. Weight decay. Here, we now study the effect of varying the level of regularization on test error. We train CIFAR10 with data-augmentation and 20% label noise on ResNet18 for weight decay coefficients λ ranging from 0 to 0.1. We train the

J. Stat. Mech. (2021) 124003

CIFAR10, 10% noise, SGD

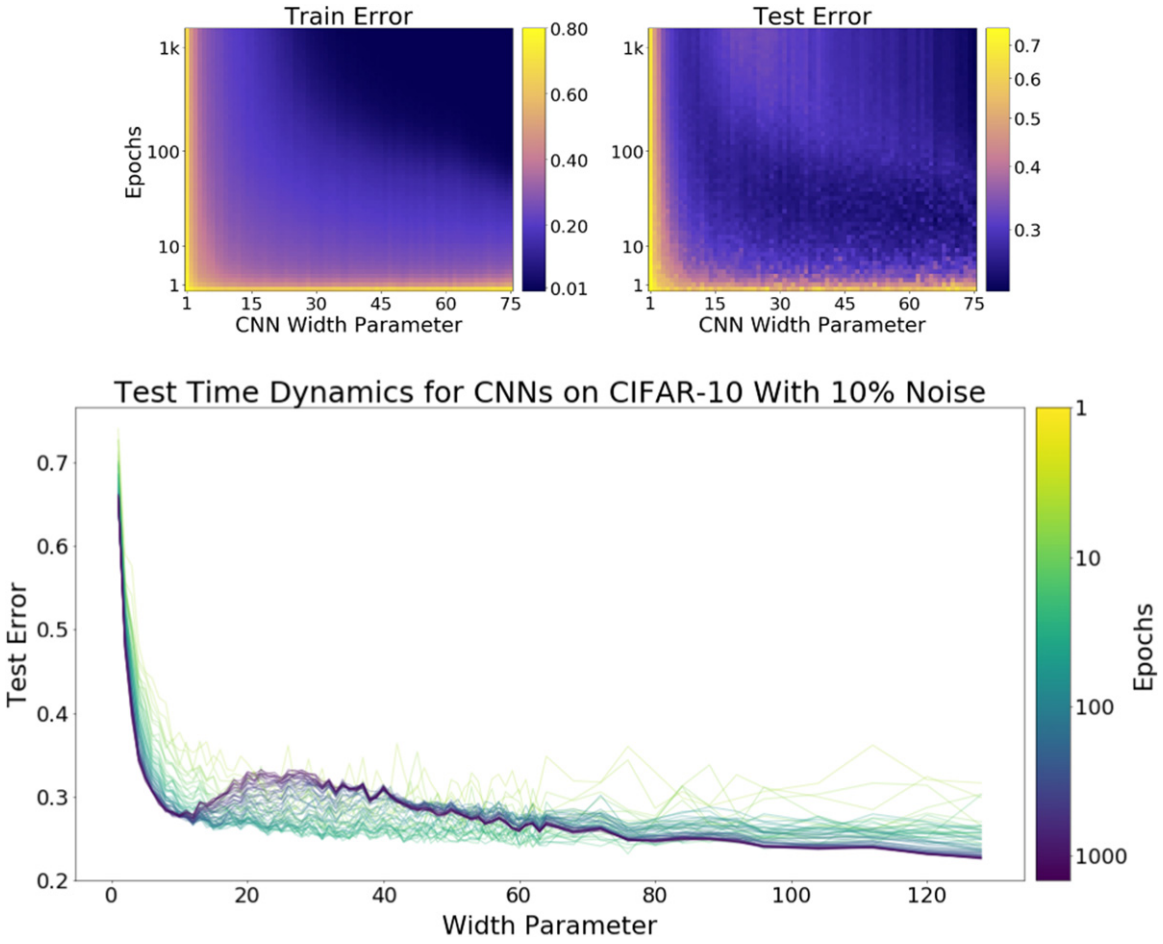

Figure 25. (Top) Train and test performance as a function of both model size and train epochs. (Bottom) Test error dynamics of the same model (CNN, on CIFAR-10 with 10% label noise, data-augmentation and SGD optimizer with learning rate $\propto 1/\sqrt{T}$).

networks using SGD + inverse-square root learning rate. Figure below shows a picture qualitatively very similar to that observed for model-wise double descent wherein

J. Stat. Mech. (2021) 124003

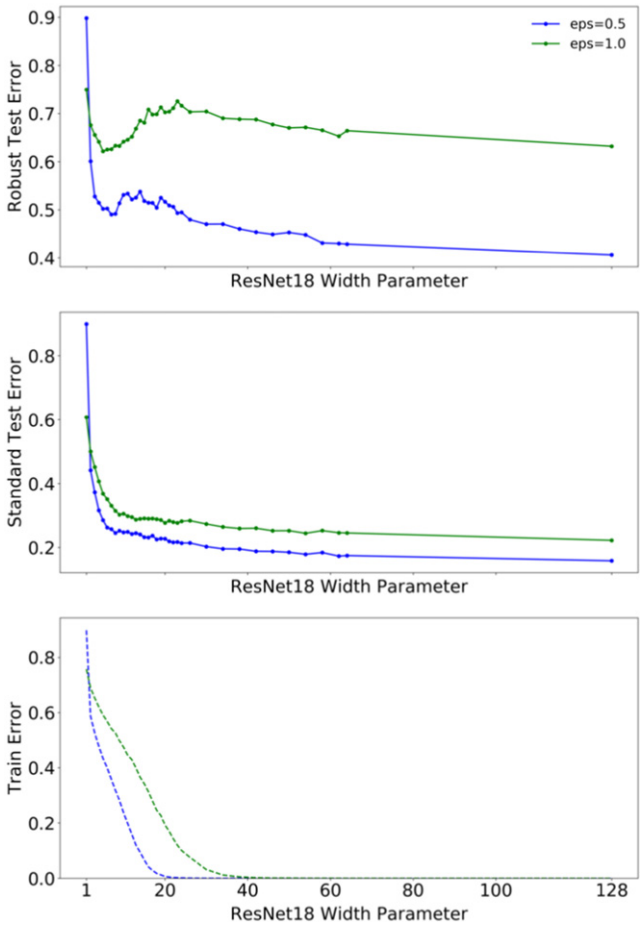

Figure 26. Model-wise double descent for adversarial training ResNet18s on CIFAR-10 (subsampled to 25k train samples) with no label noise. We train for L2 robustness of radius $\epsilon = 0.5$ and $\epsilon = 1.0$, using 10-step PGD (Goodfellow *et al* 2014, Madry *et al* 2017). Trained using SGD (batch size 128) with learning rate 0.1 for 400 epochs, then 0.01 for 400 epochs.

'model complexity' is now controlled by the regularization parameter. This confirms our generalized double descent hypothesis along yet another axis of EMC.

J. Stat. Mech. (2021) 124003

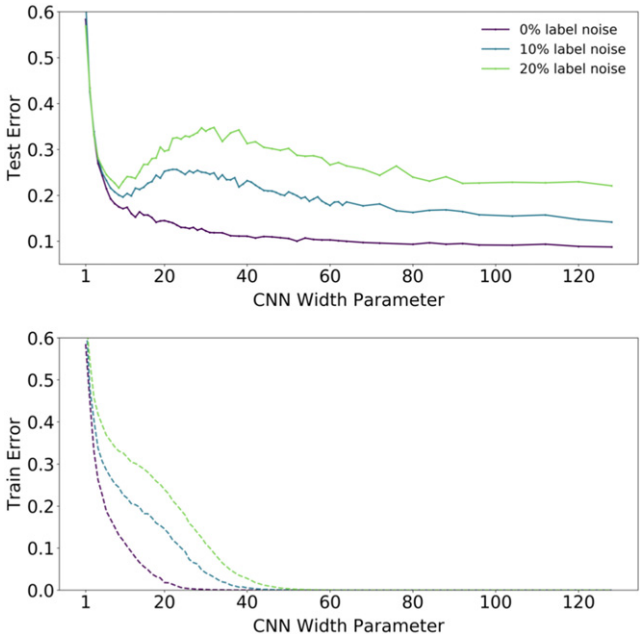

Figure 27. Effect of data augmentation: 5-layer CNNs on CIFAR-10, with data-augmentation. Optimized for 500K steps. This figure is an extension of figure 5(b) for larger models.

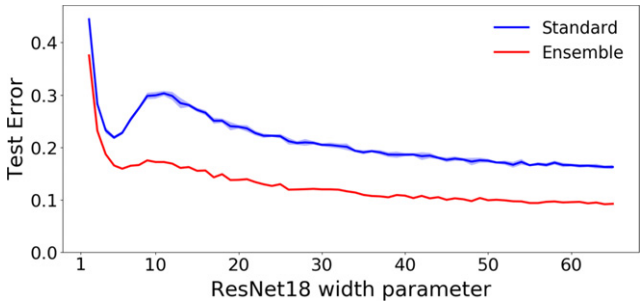

Figure 28. Effect of ensembling (ResNets, 15% label noise). Test error of an ensemble of 5 models, compared to the base models. The ensembled classifier is determined by plurality vote over the five base models. Note that emsembling helps most around the critical regime. All models are ResNet18s trained on CIFAR-10 with 15% label noise, using Adam for 4K epochs (same setting as figure 1). Test error is measured against the original (not noisy) test set, and each model in the ensemble is trained using a train set with independently-sampled 15% label noise.

E.2.3. Early stopping does not exhibit double descent.

E.2.4. Training procedure.

E.3. Ensembling

J. Stat. Mech. (2021) 124003

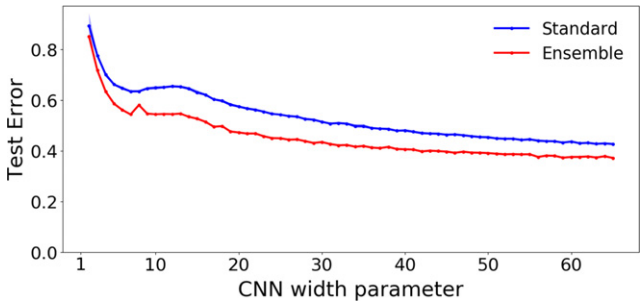

Figure 29. Effect of ensembling (CNNs, no label noise). Test error of an ensemble of five models, compared to the base models. All models are five-layer CNNs trained on CIFAR-10 with no label noise, using SGD and no data augmentation. (Same setting as figure 7).

References

Advani M S and Saxe A M 2017 High-dimensional dynamics of generalization error in neural networks (arXiv:1710.03667)

Bartlett P L, Long P M, Lugosi G and Alexander T 2019 Benign overfitting in linear regression (arXiv:1906.11300)

Belkin M, Hsu D, Ma S and Mandal S 2018 Reconciling modern machine learning and the bias-variance trade-off (arXiv:1812.11118)

Belkin M, Hsu D and Xu J 2019 Two models of double descent for weak features (arXiv:1903.07571)

Bibas K, Fogel Y and Feder M 2019 A new look at an old problem: a universal learning approach to linear regression (arXiv:1905.04708)

Cettolo M, Girardi C and Federico M 2012 Wit^3: web inventory of transcribed and translated talks *Proc. 16th Conf. European Association for Machine Translation (EAMT)* (Trento, Italy) pp 261–8

Geiger M, Arthur J, Spigler S, Gabriel F, Sagun L, d'Ascoli S, Biroli G, Hongler C and Wyart M 2019a Scaling description of generalization with number of parameters in deep learning (arXiv:1901.01608)

Geiger M, Spigler S, d'Ascoli S, Sagun L, Baity-Jesi M, Biroli G and Wyart M 2019b Jamming transition as a paradigm to understand the loss landscape of deep neural networks *Phys. Rev.* E **100** 012115

Goodfellow I J, Shlens J and Szegedy C 2014 Explaining and harnessing adversarial examples (arXiv:1412.6572)

Hastie T, Tibshirani R, Friedman J and Franklin J 2005 *The Elements of Statistical Learning* (Berlin: Springer) (https://doi.org/10.1007/b94608)

Hastie T, Montanari A, Rosset S and RyanTibshirani J 2019 Surprises in high-dimensional ridgeless least squares interpolation (arXiv:1903.08560)

He K, Zhang X, Ren S and Sun J 2016 Identity mappings in deep residual networks *European Conf. Computer Vision* (Springer) pp 630–45

Huang Y, Cheng Y, Chen D, Lee H, Ngiam J, Le Q V and Chen Z 2018 GPipe: efficient training of giant neural networks using pipeline parallelism (arXiv:1811.06965)

Krizhevsky A 2009 Learning multiple layers of features from tiny images *Technical Report* University of Toronto (https://doi.org/10.1.1.222.9220)

Krizhevsky A, Sutskever I and Hinton G E 2012 Imagenet classification with deep convolutional neural networks *Advances in Neural Information Processing Systems* pp 1097–105

Madry A, Makelov A, Schmidt L, Tsipras D and Vladu A 2017 Towards deep learning models resistant to adversarial attacks (arXiv:1706.06083)

Mei S and Montanari A 2019 The generalization error of random features regression: precise asymptotics and double descent curve (arXiv:1908.05355)

Mitra P P 2019 Understanding overfitting peaks in generalization error: analytical risk curves for l2 and l1 penalized interpolation (arXiv:1906.03667)

Muthukumar V, Vodrahalli K and Sahai A 2019 Harmless interpolation of noisy data in regression (arXiv:1903.09139)

Nakkiran P, Kaplun G, Kalimeris D, Yang T, Edelman B L, Zhang F and Barak B 2019 SGD on neural networks learns functions of increasing complexity (arXiv:1905.11604)

Opper M 1995 Statistical mechanics of learning: generalization *The Handbook of Brain Theory and Neural Networks* (Cambridge, MA: MIT Pres) pp 922–5

Opper M 2001 Learning to generalize *Front. Life* **3** 763–75

J. Stat. Mech. (2021) 124003

Ott M, Edunov S, Baevski A, Fan A, Gross S, Ng N, Grangier D and Auli M 2019 fairseq: a fast, extensible toolkit for sequence modeling *Proc. NAACL-HLT 2019: Demonstrations*

Page D 2018 How to train your resnet https://myrtle.ai/how-to-train-your-resnet-4-architecture/

Paszke A *et al* 2017 Automatic differentiation in PyTorch *NeurIPS Autodiff Workshop*

Radford A, Wu J, Child R, Luan D, Amodei D and Sutskever I 2019 Language models are unsupervised multitask learners

Rahimi A and Recht B 2008 Random features for large-scale kernel machines *Advances in Neural Information Processing Systems* pp 1177–84

Sennrich R, Haddow B and Birch A 2015 Neural machine translation of rare words with subword units (arXiv:1508.07909)

Spigler S, Geiger M, d'Ascoli S, Sagun L, Biroli G and Wyart M 2018 A jamming transition from under-to over-parametrization affects loss landscape and generalization (arXiv:1810.09665)

Szegedy C, Liu W, Jia Y, Sermanet P, Reed S, Anguelov D, Erhan D, Vincent V and Rabinovich A 2015 Going deeper with convolutions *Computer Vision and Pattern Recognition (CVPR)* (arXiv:1409.4842)

Vaswani A, Shazeer N, Parmar N, Uszkoreit J, Jones L, Gomez A N, Kaiser L and Polosukhin I 2017 Attention is all you need (arXiv:1706.03762)

Zhang C, Bengio S, Hardt M, Recht B and Vinyals O 2016 Understanding deep learning requires rethinking generalization *ICLR* (arXiv:1611.03530)

J. Stat. Mech. (2021) 124003